AIP | Applied Physics Letters

Detection of sulfur dioxide gas with graphene field effect transistor

Yujie Ren, Chaofu Zhu, Weiwei Cai, Huifeng Li, Hengxing Ji et al.

Citation: Appl. Phys. Lett. **100**, 163114 (2012); doi: 10.1063/1.4704803
View online: http://dx.doi.org/10.1063/1.4704803
View Table of Contents: http://apl.aip.org/resource/1/APPLAB/v100/i16
Published by the American Institute of Physics.

Detection of sulfur dioxide gas with graphene field effect transistor

Yujie Ren,[1,2] Chaofu Zhu,[1] Weiwei Cai,[3] Huifeng Li,[2] Hengxing Ji,[2] Iskandar Kholmanov,[2] Yaping Wu,[2,3] Richard D. Piner,[2] and Rodney S. Ruoff[2,a)]
[1]*School of Mechanical Engineering, University of Science and Technology Beijing, Beijing 100083, China*
[2]*Department of Mechanical Engineering and the Material Science and Engineering Program, The University of Texas at Austin, Austin, Texas 78712, USA*
[3]*Department of Physics, Fujian Key Laboratory of Semiconductor Materials and Applications, Xiamen University, Xiamen 361005, China*

(Received 20 February 2012; accepted 1 April 2012; published online 18 April 2012)

Graphene grown by chemical vapor deposition on a Cu foil and transferred onto a Si wafer has been used to fabricate a field effect transistor device that was used to study the sensing of SO_2 gas. It was found by *in-situ* measurements that the SO_2 strongly p-dopes the graphene and dramatically shifts its Dirac point. This effect was used to monitor the SO_2 gas. The detector can be completely reset by thermal annealing at 100 °C in high vacuum. The response and recovery of the detector are faster at higher temperatures. Moreover, the sensitivity of the SO_2 graphene detector increases proportionally with increasing temperature. © *2012 American Institute of Physics*. [http://dx.doi.org/10.1063/1.4704803]

Graphene, a two-dimensional honeycomb structure of carbon atoms, possesses unusual electronic properties that make it promising for diverse electronic applications.[1] Particularly, strong alteration of electronic properties of graphene by absorption and desorption of various gas molecules allows using it as a sensing element for gas sensor applications. Schedin *et al*. reported that a gas detector based on graphene can detect the target gas molecules at very low concentrations even down to the single molecule level.[2] Such high sensitivity can be ascribed to graphene's extremely low-noise characteristics[3] and high surface area. The mechanism of gas sensing in graphene is based on the changes of local charge carrier concentrations by adsorbed gas molecules that results in p-type or n-type doping and leads to resistance changes. Due to the high sensitivity, the electrical detection of gas molecules can be achieved even at room temperature (RT).[2,4] This is particularly important for low-temperature gas monitoring systems, for instance, for SO_2 gas detector. Reliable detection of SO_2 gas using solid electrolytes or semiconductors can only be achieved at high temperatures (450–500 °C).[5] However, because of the interference of air, accurate measurement of the graphene gas detector can only be carried out in an airtight chamber right now. Therefore, more research needs to be done to turn the gas detector into a real gas sensor.

Monitoring of SO_2 gas is important because it is one of the most common air pollutants from industrial complexes and vehicles and can cause acid rain that is harmful to plants, buildings, and human beings.[6] In this study, SO_2 is mixed with inert gas and sensed with chemical vapor deposition (CVD) grown graphene configured in a field effect transistor (FET) device. It was found that the Dirac point of graphene shifts 1.09 V/ppm maximum when the graphene FET is exposed to SO_2 gas molecules in the part-per-million (ppm) range, thus demonstrating an effective way to detect SO_2 gas. The complete recovery of the detector baseline was achieved by annealing at 100 °C in high vacuum. Because of its high response rate and simple recovery process, graphene is a promising material for the next generation of SO_2 gas sensor.

Large area graphene samples were grown on 25-μm thick copper foils (Alfa Aesar, item No. 13382) in a cold-wall CVD furnace, as described elsewhere.[7,8] Briefly, the copper foil (1 mm × 10 mm) was annealed through direct current heating (over 35 A) up to 880 °C in the vacuum chamber with base pressure of 1.0×10^{-2} Torr. The foil was kept at this temperature and exposed to methane for 10 min. The CVD process results in the growth of monolayer graphene on both sides of the copper foils. A "fish out" transfer method, which we reported before, was used to transfer graphene from Cu foils onto a Si wafer (with 280 nm thick oxide layer).[8,9] This method allows obtaining clean monolayer graphene without, e.g., PMMA residues, which is important for gas sensing applications. Micro-Raman spectroscopy (WITec Alpha 300, excitation wavelength 532 nm) was used to evaluate the quality and the number of layers of the graphene. Fig. 1 shows the optical microscope image (×20) and a typical Raman spectrum of monolayer graphene. Its sharp G band (~1580 cm^{-1}), high 2D band (~2690 cm^{-1}), a low G/2D ratio, and very low D band (~1350 cm^{-1}) indicate the good quality of our sample.[10] The optical image shows no cracks, wrinkles, or chemical residue on the surface of the graphene.

For fabrication of the graphene-based FET, two gold electrodes (5 × 5 mm) were deposited on graphene-on-Si wafer by thermal evaporation of Au wire and through a metal shadow mask (channel length: 1 mm). The graphene FET was then put into the vacuum chamber[11,12] that was connected to a 50-ppm SO_2 standard gas (volume balanced with N_2, Airgas Company). The graphene FET inside the chamber was connected to the outside measurement instruments *via* electrical feedthroughs on the vacuum chamber. In order to eliminate the initial H_2O and O_2 absorbents, the graphene SO_2 gas detector was annealed at 100 °C for 1 h and cooled down overnight to RT under high vacuum (1×10^{-9} Torr).

a)Author to whom correspondence should be addressed. Electronic mail: r.ruoff@mail.utexas.edu.

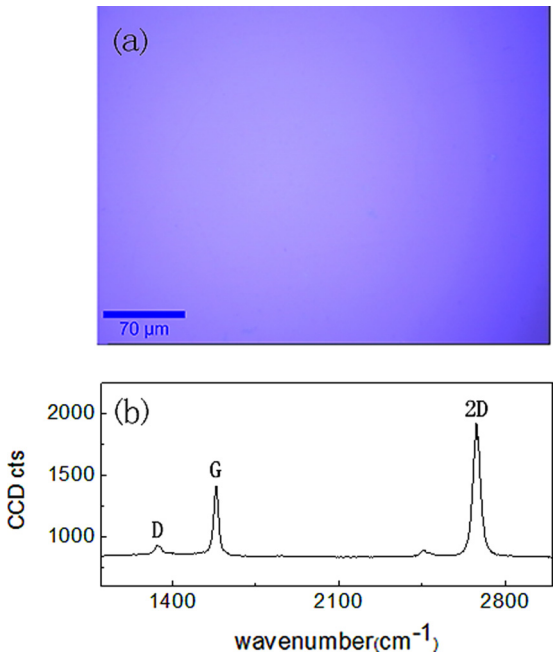

FIG. 1. (a) Optical microscope image and (b) typical Raman spectrum of the CVD grown monolayer graphene after transfer to SiO_2/Si.

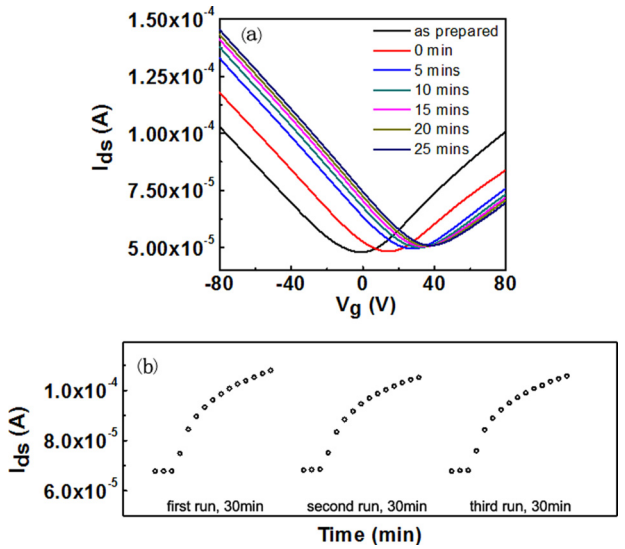

FIG. 3. The response of the graphene FET to SO_2 gas at RT. (a) Time dependence of drain-source current (I_{ds}) versus gate bias (V_g) at a drain-source bias of 2.53 V. (b) Reproducibility of the graphene FET as a SO_2 gas detector at RT for exposure to 50-ppm SO_2 for a drain-source voltage of 2.53 V and gate voltage of −50 V. The measurement time of each sample run was 30 min.

Then, a predefined volume of the 50-ppm SO_2 gas was introduced through a mass flow controller and trapped in the chamber to test the response of the graphene FET as a SO_2 gas detector. Temperature dependent gas sensing measurements were carried out in the temperature range of 40 °C–100 °C. Keithley Instruments (Keithley 6514 and 6221) were controlled by a LabVIEW program to record the measurement data automatically into a computer.

Our FET device was exposed to pure N_2 after high vacuum anneal, and the result was shown in Fig. 2 (2.0 Torr). No obvious shift of the Dirac point indicated the graphene FET had no response to N_2. During the *in-situ* exposure to SO_2, the FET curves were recorded to map the evolution of the position of the Dirac point. In Fig. 3(a), the black curve was obtained at room temperature (after annealing the sample at 100 °C for 1 h and then cooling it down to RT overnight in the vacuum chamber). The Dirac point located around zero gate bias indicates that almost all of the initial doping introduced by absorbents such as O_2 and H_2O, and other residual molecules had been removed. This clean graphene in the FET was then exposed to SO_2 gas *via* a mass flow-controller (Sierra, smart-Trak) with a 10-sccm flow for 2 min to introduce the standard 50-ppm SO_2 gas into the vacuum chamber. This process was controlled by a LabVIEW program to make sure that at every batch exactly the same volume of SO_2 gas was introduced into the chamber resulting in a pressure change from 1.0×10^{-9} Torr to 2.0 Torr. The electrical response was immediately recorded after trapping the SO_2 gas in the chamber and repeated every 2.5 min for a total time of 30 min. Fig. 3(a) shows that as SO_2 gas adsorbs on the graphene surface, it induces a shift of the curve (drain and source current (I_{ds}) versus gate bias (V_g)) to the positive side. Initially, the Dirac point is at zero gate bias (before introducing the SO_2 gas), and after 10 min exposure to the SO_2 gas, it is at about +30 V and then gradually shifts to its final position of about +35 V. First-principles calculations showed that dipolar molecules can act as donors or acceptors of electrons, respectively.[13] In our case, SO_2 acts as an acceptor and induces heavy p-doping of the graphene. The carrier density ρ introduced by the SO_2 gas deposited on the graphene sensor can be estimated by the equation $\rho = CV_D/eS = \varepsilon_0\varepsilon_r V_D/ed$, where V_D is the shift of Dirac point, e is the electron charge, ε_r is the dielectric constant of SiO_2, and d is the thickness of the SiO_2 layer. Using this equation for $V_D = 33.9$ V from Fig. 3(a), the carrier density of 2.63×10^{12} cm^{-2} corresponding to the final state for 50-ppm SO_2 at RT was obtained.

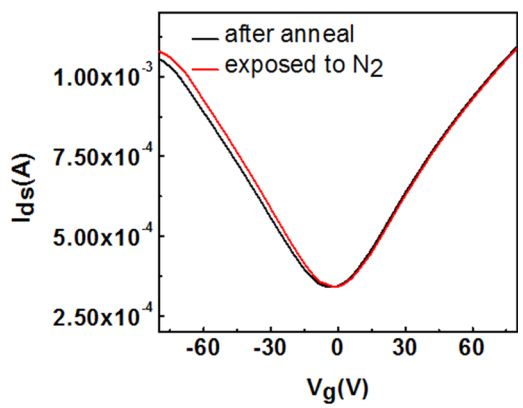

FIG. 2. The response of the graphene FET to pure N_2 gas. The drain-source voltage is 2.53 V.

Reproducibility is one of the most important features of gas sensors. It was reported graphene detectors can completely recover by heating them at 150 °C in vacuum, and repetitive exposure to certain gases showed no poisoning effects.[2] We find that annealing at 100 °C in high vacuum (1.0×10^{-9} Torr) for 1 h can remove almost all the doping of the graphene. Fig. 3(b) shows the I_{ds} response as a function of time for three sample runs at the gate bias of −50 V (drain voltage: 2.53 V). After each run, the graphene detector was

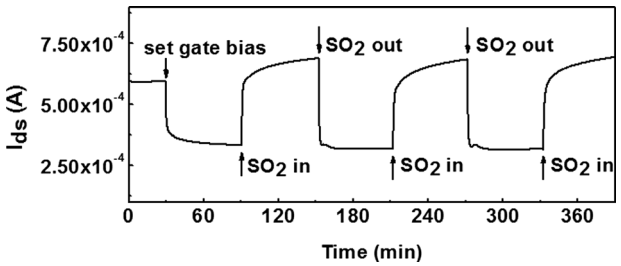

FIG. 4. The response of the graphene FET to SO_2 gas (50-ppm) at 100 °C. The drain-source voltage is 2.53 V and the gate voltage is −50 V.

heated to 100 °C in high vacuum (1.0×10^{-9} Torr) for 1 h and cooled down overnight to RT. The three curves in Fig. 3(b) show that all the adsorbed SO_2 gas molecules can be eliminated by such a treatment, and the doping is reproducible upon re-exposure to the SO_2 gas. For the SO_2 gas with same volume and concentration, the graphene detector had the same response rate and final state, thus showing good reproducibility.

For testing the detector performance at higher temperatures, the graphene FET was maintained at 100 °C and exposed to the standard 50-ppm SO_2 gas. The response of the detector was tested for three sample runs. Fig. 4 shows the time evolution of I_{ds} (drain-source current) of the detector exposed to SO_2 gas at −50 V gate bias (before setting the gate bias, its value is zero). It is clear that with the constant 2.53 V drain voltage, the I_{ds} increased rapidly as soon as the graphene FET detector was exposed to the SO_2 gas at 100 °C. The I_{ds} increased 76% in the first 2 min and then gradually approaches its final state (100%) within 30 min. The reset process is significantly faster than the response process. Within only 2 min, after the vacuum level in the chamber returned to 1.0×10^{-9} Torr, I_{ds} returns to about 98% of its initial value. With continuous pumping for 10 min (vacuum level: 1.0×10^{-9} Torr), the initial state of the graphene FET maintained at 100 °C is completely restored, and the prior exposure restore has no effect on the following measurement cycles. Fig. 4 shows how reproducibility of the graphene SO_2 detector is at 100 °C. The response and reset rate, the top and initial value of I_{ds}, are reproduced under the same conditions. Comparing Figs. 4 and 3(b), one sees that the graphene FET is more sensitive at 100 °C with faster response rate and higher response value compared to the RT measurements. In addition, the recovery of the detectors at 100 °C (10 min) is faster than at room temperature (overnight).

The graphene-FET SO_2 detector was tested to obtain the time evolution curves of I_{ds} versus V_g at different temperatures: RT, 40 °C, 60 °C, 80 °C, and 100 °C. After each measurement, the detector was reset by annealing at 100 °C (1.0×10^{-9} Torr) to eliminate the existing doping before it was used for the next measurements at another temperature. The detector was heated to the designated temperature and exposed to 50-ppm SO_2 gas, and the FET curves were recorded every 2.5 min. Experimental results shown by dots in Fig. 5(a) indicate the evolution of the Dirac point position. We now present a physical model, denoting the density of SO_2 gas molecules on the graphene surface as n and the density of SO_2 gas molecules in the gas phase as n_g, with the

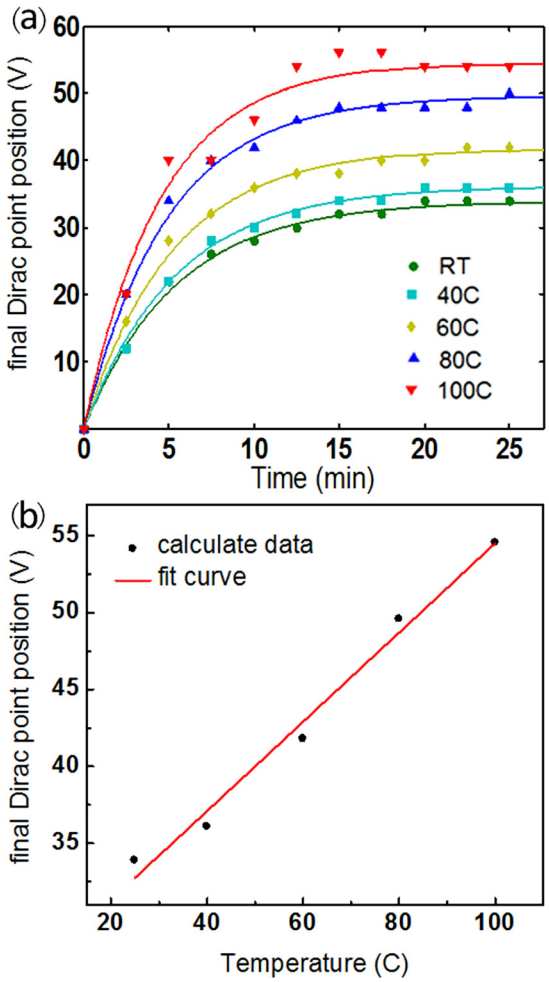

FIG. 5. (a) The shift of the graphene Dirac point at different temperatures. (b) The final Dirac point position as a function of temperature. 50-ppm SO_2 gas was used in all the experiments.

assumption that n_g in these experiments is constant. The dynamics of the adsorption/desorption rate can be expressed by the following equation:[12]

$$\frac{dn(t)}{dt} \equiv \frac{dn_{ad}}{dt} - \frac{dn_{de}}{dt} = n_g p_g - np, \tag{1}$$

where t is the exposure time of graphene to the SO_2 gas, and p_g and p are the adsorption and desorption rates, respectively. It is also assumed that the adsorption and desorption rates depend only on the temperature, and the initial state has no adsorbates ($n(t) = 0$ at $t = 0$). The density of the SO_2 molecules on the graphene surface as a function of exposure time can be obtained by solving Eq. (1),

$$n(t) = \frac{n_g p_g}{p}(1 - e^{-pt}). \tag{2}$$

Denoting the charge transfer from SO_2 to graphene as ω, the Dirac point position shift V_D as a function of exposure time t can be expressed as

$$V_D = \frac{ed\omega}{\varepsilon_0 \varepsilon_r} \cdot \frac{n_g p_g}{p}(1 - e^{-pt}) = \frac{k}{p}(1 - e^{-pt}), \tag{3}$$

where $k = \frac{ed\omega}{\varepsilon_0 \varepsilon_r} \cdot n_g p_g$. Five curves fitted to the V_D using Eq. (3) are shown in Fig. 5(a). The extracted Dirac point

position shift V_D at RT, 40 °C, 60 °C, 80 °C, and 100 °C from the fits are 33.9 V, 36.09 V, 41.8 V, 49.6 V, and 54.5 V, respectively. It is also clear from Eq. (3) that V_D depends linearly on the concentration of SO_2 absorbed on graphene, so the "shifting rate" of the Dirac point of graphene to the SO_2 concentration at RT, 40 °C, 60 °C, 80 °C, and 100 °C are 0.678 V/ppm, 0.721 V/ppm, 0.836 V/ppm, 0.992 V/ppm, and 1.09 V/ppm, respectively. Such large rates demonstrate the high sensitivity of the graphene detector to the SO_2 gas. Additionally, the final Dirac point positions depend linearly on temperature, Fig. 5(b), and the sensitivity of this detector increases as temperature increases from RT to 100 °C.

A graphene FET was fabricated and tested as a SO_2 gas detector at different temperatures by *in-situ* FET measurements in a high vacuum chamber. Adsorbed SO_2 molecules heavily p-dope graphene and thus shift its Dirac point position dramatically demonstrating that graphene FETs are viable SO_2 gas detectors. At room temperature, the Dirac point shifted 0.678 V/ppm to the positive side, and the resistance decreased about 60% at a SO_2 concentration of 50-ppm. At 100 °C, the Dirac point shifts 1.09 V/ppm to the positive side, and resistance decreased over 100% at a SO_2 concentration of 50-ppm. The detector reset time is quite long at lower temperatures, but it significantly decreases with increasing temperature (only 10 min at 100 °C). The sensitivity of the SO_2 graphene detector increased linearly between RT and 100 °C.

Support from the China Scholarship Council to Yujie Ren and Yaping Wu is greatly appreciated.

[1]M. C. Lemme, T. J. Echtermeyer, M. Baus, and H. Kurz, IEEE Electron Device Lett. **28**(4), 282 (2007); Y. Zhu, S. Murali, W. Cai, X. Li, J. W. Suk, J. R. Potts, and R. S. Ruoff, Adv. Mater. **22**(35), 3906 (2010); W. Cai, A. L. Moore, Y. Zhu, X. Li, S. Chen, L. Shi, and R. S. Ruoff, Nano Lett. **10**(5), 1645 (2010); K. S. Novoselov, A. K. Geim, S. V. Morozov, D. Jiang, Y. Zhang, S. V. Dubonos, I. V. Grigorieva, and A. A. Firsov, Science **306**(5296), 666 (2004).
[2]F. Schedin, A. K. Geim, S. V. Morozov, E. W. Hill, P. Blake, M. I. Katsnelson, and K. S. Novoselov, Nature Mater. **6**(9), 652 (2007).
[3]S. Qinghui, L. Guanxiong, D. Teweldebrhan, A. A. Balandin, S. Rumyantsev, M. S. Shur, and Y. Dong, IEEE Electron Device Lett. **30**(3), 288 (2009); E. Massera, V. La Ferrara, M. Miglietta, T. Polichetti, I. Nasti, and G. Di Francia, Chim. Oggi **29**(1), 39 (2011).
[4]Y. Dan, Y. Lu, N. J. Kybert, Z. Luo, and A. T. Johnson, Nano Lett. **9**(4), 1472 (2009); G. Ko, H. Y. Kim, J. Ahn, Y. M. Park, K. Y. Lee, and J. Kim, Curr. Appl. Phys. **10**(4), 1002 (2010).
[5]Y. Shimizu, N. Matsunaga, T. Hyodo, and M. Egashira, Sens. Actuators B **77**(1), 35 (2001); Y. Uneme, S. Tamura, T. Kawato, and N. Imanaka, Electrochem. Solid-State Lett. **14**(7), J38 (2011).
[6]G. J. S. Bluth, S. D. Doiron, C. C. Schnetzler, A. J. Krueger, and L. S. Walter, Geophys. Res. Lett. **19**(2), 151 (1992); V. Ramanathan, P. J. Crutzen, J. T. Kiehl, and D. Rosenfeld, Science **294**(5549), 2119 (2001).
[7]W. W. Cai, R. D. Piner, Y. W. Zhu, X. S. Li, Z. B. Tan, H. C. Floresca, C. L. Yang, L. Lu, M. J. Kim, and R. S. Ruoff, Nano Res. **2**(11), 851 (2009); S. S. Chen, W. W. Cai, R. D. Piner, J. W. Suk, Y. P. Wu, Y. J. Ren, J. Y. Kang, and R. S. Ruoff, Nano Lett. **11**(9), 3519 (2011); W. Cai, R. D. Piner, F. J. Stadermann, S. Park, M. A. Shaibat, Y. Ishii, D. Yang, A. Velamakanni, S. J. An, M. Stoller, J. An, D. Chen, and R. S. Ruoff, Science **321**(5897), 1815 (2008); W. W. Cai, Y. W. Zhu, X. S. Li, R. D. Piner, and R. S. Ruoff, Appl. Phys. Lett. **95**(12), 123115 (2009).
[8]X. Li, W. Cai, J. An, S. Kim, J. Nah, D. Yang, R. Piner, A. Velamakanni, I. Jung, E. Tutuc, S. K. Banerjee, L. Colombo, and R. S. Ruoff, Science **324**(5932), 1312 (2009).
[9]X. Li, W. Cai, I. H. Jung, J. H. An, D. Yang, A. Velamakanni, R. Piner, L. Colombo, and R. S. Ruoff, ECS Trans. **19**(5), 41 (2009).
[10]A. Ferrari, Solid State Commun. **143**(1–2), 47 (2007); A. C. Ferrari, J. C. Meyer, V. Scardaci, C. Casiraghi, M. Lazzeri, F. Mauri, S. Piscanec, D. Jiang, K. S. Novoselov, S. Roth, and A. K. Geim, Phys. Rev. Lett. **97**(18), 187401 (2006); D. Graf, F. Molitor, K. Ensslin, C. Stampfer, A. Jungen, C. Hierold, and L. Wirtz, Solid State Commun. **143**(1–2), 44 (2007).
[11]Y. Ren, S. Chen, W. Cai, Y. Zhu, C. Zhu, and R. S. Ruoff, Appl. Phys. Lett. **97**(5), 053107 (2010).
[12]S. Chen, W. Cai, D. Chen, Y. Ren, X. Li, Y. Zhu, and R. S. Ruoff, New J. Phys. **12**(12), 125011 (2010).
[13]O. Leenaerts, B. Partoens, and F. M. Peeters, Phys. Rev. B **77**(12), 125416 (2008).